Optical Absorption and Reflection Studies of $Tl_4InGa_3S_8$ Layered Single Crystals

K. Goksen, N.M. Gasanly* and H. Ozkan

Department of Physics, Middle East Technical University, 06531 Ankara, Turkey

(Received May 10, 2007)

The optical properties of $Tl_4InGa_3S_8$ layered single crystals have been studied by means of transmission and reflection measurements in the wavelength region between 400 and 1100 nm. The analysis of the room temperature absorption data revealed the presence of both optical indirect and direct transitions with band gap energies of 2.40 and 2.61 eV, respectively. Transmission measurements carried out in the temperature range of 10–300 K revealed the rate of change of the indirect band gap with temperature as $\gamma = -6.0 \times 10^{-4}$ eV/K. The absolute zero value of the band gap energy was obtained as $E_{gi}(0) = 2.52$ eV. The dispersion of the refractive index is discussed in terms of the Wemple–DiDomenico single-effective-oscillator model. The refractive index dispersion parameters: oscillator energy, dispersion energy, oscillator strength, and zero-frequency refractive index were found to be 5.07 eV, 26.67 eV, 8.82×10^{13} m^{-2}, and 2.50, respectively.

PACS numbers: 78.20.Ci, 78.40.–q, 78.40.Fy

1. Introduction

$Tl_4InGa_3S_8$ is the compound that belongs to the layered semiconductors group. This crystal is formed from $TlGaS_2$ crystal replacing a quarter of gallium atoms by indium atoms [1, 2]. The crystal lattice has two-dimensional layers arranged parallel to the (001) plane. The bonding between Tl and S atoms in $Tl_4InGa_3S_8$ is of an interlayer type whereas the bonding between (In)Ga and S is of an intralayer type.

Optical and photoelectrical properties of $TlGaS_2$ crystals were studied in Refs. [3–8]. The fundamental absorption edges are formed by indirect and direct transitions with $E_{gi} = 2.38$ eV and $E_{gd} = 2.53$ eV [3]. A high photosensitivity in the visible range of spectra, high birefringence in conjunction with a wide

*corresponding author; e-mail: nizami@metu.edu.tr

transparency range of 0.5–14 μm make these crystals useful for optoelectronic applications [8]. Previously, we studied the optical properties of the Tl_2InGaS_4 crystals [9]. The analysis of the room temperature absorption data revealed the presence of both optical indirect and direct transitions with band gap energies of 2.35 and 2.54 eV, respectively. From transmission measurements carried out in the temperature range of 10–300 K, the rate of change of the indirect band gap with temperature was found to be $\gamma = -4.70 \times 10^{-4}$ eV/K.

The purpose of this study is to present the optical constants of $Tl_4InGa_3S_8$ crystal in the wavelength range of 400–1100 nm. The room temperature reflectance and transmittance data is analyzed to identify the refractive index, oscillator energy and strength, dispersion energy, zero-frequency dielectric constant, and refractive index. The determination of these optical constants is expected to widespread the available physical information. The rate of change of the indirect band gap with temperature is evaluated from temperature dependence of transmission spectra in 10–300 K range.

2. Experimental details

Single crystals of $Tl_4InGa_3S_8$ were grown by the Bridgman method from stoichiometric melt of starting materials. The resulting ingots (green-yellow in color) showed good optical quality and freshly cleaved surfaces were mirror-like. The chemical composition of $Tl_4InGa_3S_8$ crystals, shown in Fig. 1, was determined by energy dispersive spectroscopic analysis (EDSA) using JSM-6400 Electron Microscope. The composition of the studied samples (Tl:In:Ga:S) was estimated as 26.1:6.1:19.0:48.8, respectively. Moreover, EDSA indicates that carbon, oxygen, and silicon impurities are present in $Tl_4InGa_3S_8$ crystals.

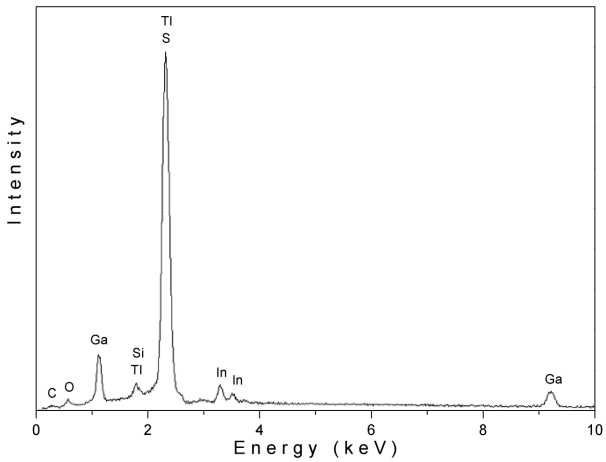

Fig. 1. Energy dispersive spectroscopic analysis of $Tl_4InGa_3S_8$ crystal.

Transmission and reflection measurements were carried out in the 400–1100 nm wavelength region with a Shimadzu UV-1201 model spectrophotometer by using 20 W halogen lamp, holographic grating, and silicon photodiode. For room temperature reflection experiments we used the specular reflectance measurement attachment with 5° incident angle. The resolution of the spectrophotometer was 5 nm. An Advanced Research Systems, Model CSW-202 closed-cycle helium cryostat was used to cool the sample from room temperature down to 10 K.

3. Results and discussion

For $Tl_4InGa_3S_8$ single crystals, the transmittance (T) and reflectivity (R) spectra were measured in 400–1100 nm wavelength (λ) range (Fig. 2). The reflectivity of the material with refractive index n and absorption coefficient α is given by [10]:

$$R = \frac{(n-1)^2 + \left(\frac{a\lambda}{4\pi}\right)^2}{(n+1)^2 + \left(\frac{a\lambda}{4\pi}\right)^2}. \tag{1}$$

The transmittance is represented by the expression

$$T = \frac{(1-R)^2 \exp(-\alpha d)}{1 - R^2 \exp(-2\alpha d)}, \tag{2}$$

where d is the sample thickness. By using these relations, n and α can be determined from the measurements of reflectivity and transmittance.

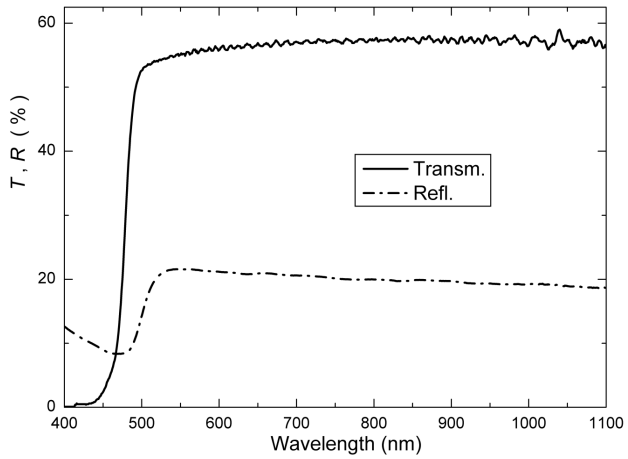

Fig. 2. The spectral dependence of transmittance and reflectivity for $Tl_4InGa_3S_8$ crystal at $T = 300$ K.

The reflectivity is measured using specimens with natural cleavage planes and a thickness such that $\alpha d \gg 1$. The sample is then reduced in thickness (by repeated cleaving using transparent adhesive tape) until it is convenient for

transmission measurements. The thickness is determined using transmission interference fringes at wavelength slightly longer than the intrinsic absorption edge, i.e., in a region with relatively high transmission (Fig. 2). For this purpose, the long wavelength value of the refractive index $n = 2.52$, obtained from the reflection measurements was used. In most cases the sample thickness was about 10 μm for room temperature transmission measurements.

The dependence of absorption coefficient on photon energy is analyzed in the high absorption regions to obtain the detailed information about the energy band gaps. The absorption coefficient α and photon energy can be related by [10]:

$$(\alpha h\nu) = A(h\nu - E_{\mathrm{g}})^{p}. \tag{3}$$

In this equation, A is a constant that depends on the transition probability and p is an index that characterizes the optical absorption process and it is theoretically equal to 2 and 1/2 for indirect and direct allowed transitions, respectively.

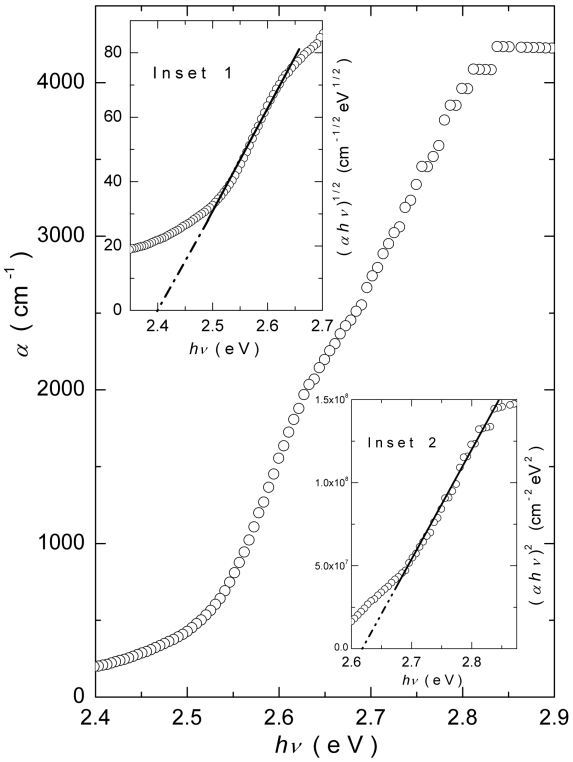

Fig. 3. The variation of absorption coefficient as a function of photon energy at $T = 300$ K. Insets 1 and 2 represent the dependences of $(\alpha h\nu)^{1/2}$ and $(\alpha h\nu)^{2}$ on photon energy, respectively.

Figure 3 shows the calculated room temperature absorption coefficient α for $Tl_4InGa_3S_8$ crystal in the photon energy range 2.40–2.85 eV. It was revealed that

α changes from 200 to 4230 cm^{-1} with increasing photon energy from 2.40 to 2.85 eV. Analysis of the experimental data shows that the absorption coefficient is proportional to $(h\nu - E_{\rm g})^p$ with $p = 2$ and $1/2$ for ranges 2.50–2.65 eV and 2.68–2.85 eV, respectively. Insets 1 and 2 of Fig. 3 display the dependences of $(\alpha h\nu)^{1/2}$ and $(\alpha h\nu)^2$ on photon energy $h\nu$, respectively. The circles are the experimental data that were fitted to a linear equation (the solid lines) for finding the band gaps. The linear dependences were observed for the relations $(\alpha h\nu)^{1/2}$ and $(\alpha h\nu)^2$ versus $h\nu$. This suggests the realization of indirect and direct allowed transitions for $Tl_4InGa_3S_8$ crystal over the ranges 2.50–2.65 eV and 2.68–2.85 eV, respectively. The extrapolations of the straight lines down to $(\alpha h\nu)^{1/2} = 0$ and $(\alpha h\nu)^2 = 0$ give the values of indirect and direct band gap energies $E_{\rm gi} = 2.40 \pm 0.02$ eV and $E_{\rm gd} = 2.61 \pm 0.02$ eV, respectively.

Figure 4 shows the transmission spectra for $Tl_4InGa_3S_8$ crystal registered in the temperature range of 10–300 K. Since the thin layered samples were very fragile, they broke into pieces at low temperatures. Therefore, the low-temperature measurements were carried out on thick samples (about 350 μm). As a consequence, we were able to analyze the temperature dependence of indirect energy band gap ($E_{\rm gi}$) only. Technical reasons did not allow a direct measurement of the reflection at low temperatures. Therefore, for the calculation of absorption coefficient α, the spectral dependence of room temperature reflectivity was uniformly shifted in energy according to the blue shift of the absorption edge.

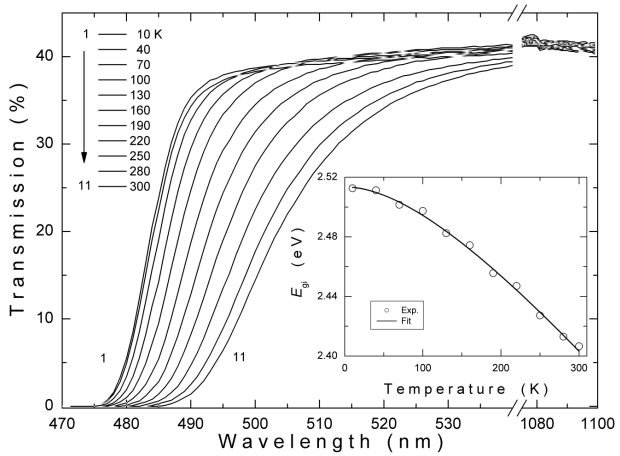

Fig. 4. The spectral dependence of transmittance for $Tl_4InGa_3S_8$ crystal in the temperature range of 10–300 K. Inset: the indirect band gap energy as a function of temperature. The solid line represents the fit using Eq. (4).

The obtained value of indirect transition energy gap decreases with increasing temperature as illustrated in the inset of Fig. 4. Namely, it shifts from 2.51 to 2.41 eV as temperature increases from 10 to 300 K. The temperature dependence

of the energy band gap can be represented by the relation [10]:

$$E_{\rm gi}(T) = E_{\rm gi}(0) + \frac{\gamma T^2}{T+\beta}, \tag{4}$$

where $E_{\rm gi}(0)$ is the absolute zero value of the band gap, $\gamma = {\rm d}E_{\rm gi}/{\rm d}T$ is the rate of change of the band gap with temperature and β is approximately the Debye temperature. The data of the $E_{\rm gi} - T$ dependence (inset of Fig. 4) were fitted using Eq. (4). The fitting is represented by the solid line that revealed the fitting parameters as $E_{\rm gi}(0) = 2.52$ eV, $\gamma = -6.0 \times 10^{-4}$ eV/K and $\beta = 190$ K. It should be noted that the Debye temperature for $Tl_4InGa_3S_8$ crystal was found to be $\beta = 183$ K estimated by Lindemann's melting rule [11].

The refractive index n as a function of wavelength, calculated using Eqs. (1) and (2), is shown in Fig. 5. The refractive index in the energy region of $h\nu < E_{\rm g}$

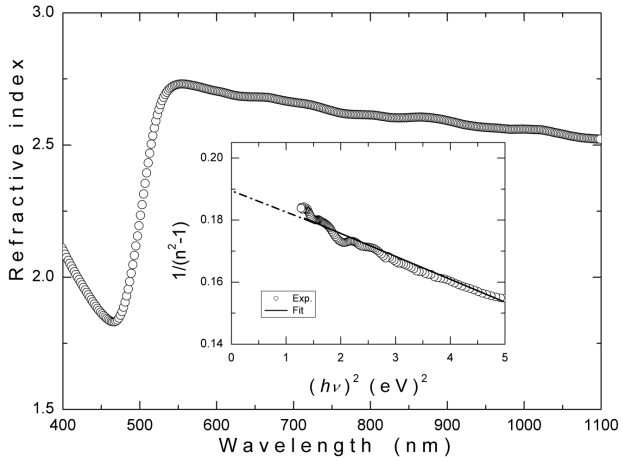

Fig. 5. The dependence of refractive index on the wavelength for $Tl_4InGa_3S_8$ crystal. Inset: Plot of $(n^2-1)^{-1}$ versus $(h\nu)^2$. The solid line represents the fit using Eq. (5).

gradually decreases from 2.73 to 2.52 with increasing wavelength in the range 555–1100 nm. The long wavelength value of refractive index is consistent with the values 2.7 ($\lambda = 800$ nm), 2.6 ($\lambda = 1100$ nm), and 2.6 ($\lambda = 1100$ nm) reported for $TlInS_2$ [12], $TlGaS_2$ [13], and Tl_2InGaS_4 [9] single crystals, respectively.

The dispersive refractive index data in $h\nu < E_{\rm g}$ range were analyzed according to the single-effective-oscillator model proposed by Wemple and DiDomenico [14, 15]. This model was successfully applied to the experimental data for the ternary $TlGaSe_2$ and $TlGaS_2$ layered crystals [16, 13]. The refractive index is related to photon energy through the relationship

$$n^2(h\nu) = 1 + \frac{E_{\rm so}E_{\rm d}}{E_{\rm so}^2 - (h\nu)^2}, \tag{5}$$

where $E_{\rm so}$ is the single oscillator energy and $E_{\rm d}$ is the dispersion energy. Plotting $(n^2-1)^{-1}$ versus $(h\nu)^2$ allows the determination of the oscillator parameters by

fitting a linear function to the lower energy range (1.15–2.24 eV). The fitting of the above reported function is presented in the inset of Fig. 5. The zero-frequency refractive index n_0 is estimated from Eq. (5), i.e. according to the expression $n_0^2 = 1 + E_\mathrm{d}/E_\mathrm{so}$.

The values of the parameters E_so and E_d were calculated from the slope and the intersection with y-axis of the straight line (inset of Fig. 5) as 5.07 eV and 26.67 eV, respectively. Moreover, the values of zero-frequency dielectric constant $\varepsilon_0 = n_0^2 = 6.26$ and refractive index $n_0 = 2.50$ were evaluated by means of Eq. (5). The oscillator energy E_so is an "average" gap energy and, to fair approximation, it is associated empirically with the lowest direct band gap E_gd by the relation $E_\mathrm{so} \approx 2E_\mathrm{gd}$ [17–20]. The ratio $E_\mathrm{so}/E_\mathrm{gd}$ for $Tl_4InGa_3S_8$ crystal determined in this study was found to be 1.94.

The refractive index n can also be analyzed to determine the oscillator strength S_so for $Tl_4InGa_3S_8$ crystal. The refractive index is represented by a single Sellmeier oscillator at low energies [21]:

$$\frac{n_0^2 - 1}{n^2 - 1} = 1 - \left(\frac{\lambda_\mathrm{so}}{\lambda}\right)^2, \tag{6}$$

where λ_so is the oscillator wavelength. Rearranging Eq. (6) gives [18]:

$$(n^2 - 1)^{-1} = \frac{1}{S_\mathrm{so}\lambda_\mathrm{so}^2} - \frac{1}{S_\mathrm{so}\lambda^2}. \tag{7}$$

Here, $S_\mathrm{so} = (n_0^2 - 1)/\lambda_\mathrm{so}^2$. The values of S_so and λ_so calculated from $(n^2 - 1)^{-1}$ versus λ^{-2} plot were found to be 8.82×10^{13} m^{-2} (135.67 eV^2) and 2.44×10^{-7} m, respectively. The obtained value of oscillator strength is of the same order as those obtained for ZnS, ZnSe, Ag_2S, $GeSe_2$, and $TlGaS_2$ crystals [15, 22, 19, 13].

4. Conclusions

The optical transmission and reflection of $Tl_4InGa_3S_8$ crystals were measured over the 400 and 1100 nm spectral region in order to derive the absorption coefficient and refractive index. The analysis of the room temperature absorption data revealed the coexistence of indirect and direct transitions in $Tl_4InGa_3S_8$ crystals with energy band gaps of 2.40 and 2.61 eV, respectively. The absorption edge was observed to shift toward lower energy values as temperature increases from 10 to 300 K. The data were used to calculate the indirect energy band gap of the crystal as a function of temperature. The rate of the change of the indirect band gap with temperature was estimated as $\gamma = -6.0 \times 10^{-4}$ eV/K. The absolute zero value of the band gap energy was found to be $E_\mathrm{gi}(0) = 2.52$ eV. The refractive index dispersion data were analyzed using the Wemple–DiDomenico single-effective-oscillator model. As a result, the oscillator energy, dispersion energy, oscillator strength, and zero-frequency refractive index were determined.

References

[1] D. Muller, H. Hahn, *Z. Anorg. Allg. Chem.* **438**, 258 (1978).

[2] K.A. Yee, A. Albright, *J. Am. Chem. Soc.* **113**, 6474 (1991).

[3] M. Hanias, A. Anagnostopoulos, K. Kambas, J. Spyridelis, *Mater. Res. Bull.* **27**, 25 (1992).

[4] A. Kato, M. Nishigaki, N. Mamedov, M. Yamazaki, S. Abdullaeva, E. Kerimova, H. Uchiki, S. Iida, *J. Phys. Chem. Solids* **64**, 1713 (2003).

[5] I.M. Ashraf, *J. Phys. Chem.* **108**, 10765 (2004).

[6] O. Karabulut, M. Parlak, G.M. Mamedov, *J. Alloys Comp.* **429**, 50 (2007).

[7] S. Kashida, Y. Yanadori, Y. Otaki, Y. Seki, A.M. Panich, *Phys. Status Solidi A* **203**, 2666 (2006).

[8] K.R. Allakhverdiev, *Solid State Commun.* **111**, 253 (1999).

[9] K. Goksen, N.M. Gasanly, H. Ozkan, *J. Phys., Condens. Matter* **19**, 256210 (2007).

[10] J.I. Pankove, *Optical Processes in Semiconductors*, Prentice-Hall, New Jersey 1971.

[11] J.R. Drabble, H.J. Goldsmid, *Thermal Conduction in Semiconductors*, Pergamon, Oxford 1961.

[12] J.A. Kalomiros, A. Anagnostopoulos, *Phys. Rev. B* **50**, 7488 (1994).

[13] A.F. Qasrawi, N.M. Gasanly, *Phys. Status Solidi A* **202**, 2501 (2005).

[14] S.H. Wemple, M. DiDomenico, *Phys. Rev. B* **3**, 1338 (1971).

[15] S.H. Wemple, M. DiDomenico, *Phys. Rev. Lett.* **23**, 1156 (1969).

[16] M.M. El-Nahass, M.M. Sallam, S.A. Rahman, E.M. Ibrahim, *Solid State Sci.* **8**, 488 (2006).

[17] K. Tanaka, *Thin Solid Films* **66**, 271 (1980).

[18] F. Yakuphanoglu, A. Cukurovali, I. Yilmaz, *Physica B* **351**, 53 (2004); *Physica B* **353**, 210 (2004).

[19] E. Marguez, P. Nagels, J.M. Gonzalez-Leal, A.M. Bernal-Oliva, E. Sleeckx, R. Callaerts, *Vacuum* **52**, 55 (1999).

[20] E. Marguez, A.M. Bernal-Oliva, J.M. Gonzalez-Leal, R. Pricto-Alcon, A. Ledesma, R. Jimenez-Garay, I. Martil, *Mater. Chem. Phys.* **60**, 231 (1999).

[21] A.K. Walton, T.S. Moss, *Proc. Phys. Soc.* **81**, 509 (1963).

[22] M.M. El-Nahass, A.M.M. Farag, E.M. Ibrahim, S.A. Rahman, *Vacuum* **72**, 453 (2004).